Measurements and Analysis on Dynamic Off-Body Radio Channels at UWB Frequencies

Timo Kumpuniemi, Juha-Pekka Mäkelä, Matti Hämäläinen, Kamya Yekeh Yazdandoost, Jari Iinatti

Centre for Wireless Communications
University of Oulu
Oulu, Finland
forename.surname@oulu.fi

***Abstract*—This paper presents measurements on dynamic off-body radio channels in an ultra wideband frequency range for wireless body area network communications focusing on the human body shadowing effect. Measurements were conducted in an anechoic chamber at a bandwidth of 2-8 GHz by using a vector network analyzer. The investigation was performed at several discrete frequencies. Two planar prototype antennas were utilized (dipole and double loop). Six on-body antenna locations were applied and one off-body site. At first, ten frequencies were examined at two links, and the path loss values and standard deviations were determined. Second, all the links were considered at three discrete frequencies. The mean path losses varied between 47.6-69.4 dB, at human-pole distances on the average of 2m. The maximum recorded value was 101.7 dB. No clear difference was noted between the antennas. The usage of dipole and double loop as a link antenna pair has no remarkable effect compared to the case when all the antennas are similar.**

Keywords—human body shadowing effect; wireless body area network; dynamic channel; ultra wideband.

I. INTRODUCTION

The rapid development of electronics together with the increasing computational performance of electronic devices is opening new potential for application development. Also, the size of the devices is constantly decreasing giving the possibility for locating the devices in new surroundings. This is related to the concept of Internet of Things (IoT), where small sensors will be used to monitor different parameters in our everyday life.

The soon to be implemented fifth generation wireless systems (5G) has one specific focus on the IoT. Furthermore, the currently highly speeding up research topic of the sixth generation (6G) wireless technology will expand the IoT framework even more. Both 5G and 6G will provide a vast playground to utilize IoT sensors in many fields of the everyday life of the society and individuals. In the society, applications can be found in public infrastructures, industry, factories, and commercial field in, e.g., shopping centers and supermarkets. Furthermore, it can be used in, e.g., monitoring residences, personal properties, vehicles, free-time apartments, and vessels.

One specific application area for IoT can be found in Wireless Body Area Networks (WBANs). Small-sized sensors can be installed not only on a body of a human, but also on the "bodies" of buildings, vehicles or industrial machines. The WBAN sensors form up a network and transmit the collected data through an access point to be connected to the outside world. For an individual, WBANs provide a method to follow up their personal well-being and health parameters e.g. with a cloud-based service. When WBANs are used with humans, the use-cases can be classically divided firstly into on-body communications, where sensors are placed on the human body. Secondly, in off-body communications, one or more sensors are located in the close vicinity of the bodies. Thirdly, in in-body communications the sensors can be situated even inside the bodies [1].

In the well-being sector, this is reality as per today. Several already commercialized products are available. With these, the user can be aware of one's heartbeat, effectiveness of a physical training etc. Furthermore, daily physical activity and quality of sleep can be monitored and analyzed with countless of applications.

In many countries, the demographic distribution of the citizens is changing as the population is ageing [2]. This is from one side due to the progress in medicine as more and new diseases can be treated increasing the expected life-time. On the other side, in the countries with this development, also the birth rates and the average family sizes are decreasing.

The abovementioned progress sets new and large challenges to the medical sectors. The organization and solving the increasing demand of the services needed, in a more cost effective manner is currently under vivid discussion among many nations.

One solution discussed for some years is to utilize WBANs in the professional medical care as well. In hospitals and medical wards, WBANs can ease up the work load of the staff as the patients can be monitored remotely at medical wards and their homes. Remote monitoring at homes decreases the time that the patients have to spend in medical wards as they can be called to a doctor's appointment when needed. The well-being of life of the patients is increased as they can spend more time and live longer in their homes. The lack of wires provides comfort both for the patients and the medical staff. The quality of treatment is improved, as the small sensors can measure the body parameters constantly, instead of infrequently taken tests in a medical laboratory.

The Ultra Wideband (UWB) technology provides a highly suitable option to WBANs. An UWB signal has low

This work has been partly funded by the Academy of Finland project 6Genesis Flagship (grant no. 318927).

transmission power making it suitable for short distance communications. The power density level of the signal is very low, often below the level of the noise density, causing a minimum specific absorption rate exposure to humans, other telecommunication systems and medical devices nearby. On the other side, it is very tolerant to interference originating from other systems. Accurate positioning can be achieved with it, as well. The simple and small structure of the transceivers have low cost together with low power consumption [3,4]. In 2012, the standard IEEE802.15.6 was released to be applied with WBANs. UWB is one of the focal waveforms defined to be used in on-, off-, and in-body communications [5].

This paper reports the results of measurements on dynamic UWB off-body radio channels. The measurements are carried out in an anechoic chamber by using a vector network analyzer at a frequency band of 2-8 GHz. Two planar prototype antennas are used: dipole and double loop.

The focus of this paper is to extract information of the human body shadowing effect on off-body radio channels. The paper extends the knowledge on UWB off-body channels reported in a static case in [6,7,8] and dynamic case in [8,9]. The work is related to a larger measurement campaign, whose other results are reported in, e.g., [7,9,10,12].

The structure of the paper is as follows. Section II describes the used facilities. Section III explains the measurement scenarios conducted. Section IV defines the data manipulation method and the selection of frequencies. In section V, results are presented and discussed. Section VI conclusion and plans for the future work are given.

II. Measurement Facilities

A. Anechoic Chamber and Person Under Test

The utilized anechoic chamber had a floor size of 2.45 m by 3.65 m and was built using movable absorber blocks in an electromagnetic compatibility room. A male at his late twenties with a height of 183 cm and weight of 95 kg was serving as a test person. Normal cotton jeans and a T-shirt were worn. Shoes and metal containing particles, e.g., belt, ring, mobile phone, coins, were absent.

B. VNA and Antennas

A four-port VNA by Rohde & Schwarz ZVA8 was used. The VNA was set to sweep the 2-8 GHz frequency band and to collect 1601 points in the band. The sweep time was set to 288.18 ms, intermediate frequency (IF) bandwidth 100 kHz and the transmit power +10 dBm. For each link, 100 sweeps were recorded, both forward and reverse directions. Due to the delay of saving the data to the VNA, the duration for recording 100 sweeps was in practice approx. 90 s, giving a sample interval in one specific frequency of approx. 0.9 s.

Two planar, in-house fabricated prototype antennas were applied in the measurements; dipole and double loop antennas. The antennas are shown in Fig. 1, where the ruler is in centimeters. The antenna structures, dimensions and simulated performances, together with measured free space radiation patterns are available in [13-15].

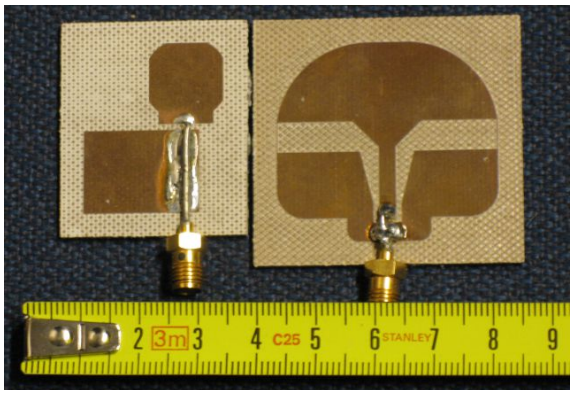

Figure 1. Utilized antennas: dipole (left) and double loop (right).

III. Measurement Scenarios

For the measurements, six on-body locations were selected as depicted in Fig. 2a). The locations lie at the left ear (LE), right ear (RE), left shoulder (LS), right wrist (RW), left wrist (LW) and left ankle (LA). The off-body node was placed on a pole at the height of 2 meters and a distance of 2 meters from the initial position of the test person. Cases, when all antennas are of uniform type (all either dipoles or double loops) and cases when they are mixed (two dipoles, two double loops) were measured. For LW, the antennas in the mixed case were situated on the dorsal side of the wrist, whereas in the uniform case they were on the palmar side, as with RW in all cases. The positions and antenna types are collected in Table I.

For on-body antenna fixings, elastic bands and paper tape were used. Between the antenna and the body, a 20 mm piece of ROHACELL 31HF was installed. In [12,13], it was noted, that this distance provides both a good antenna matching and low channel path loss at the same time.

In the beginning of a measurement, the test person was standing still at a distance of 2 m from the pole, facing towards it, as shown in Fig. 2b). During a measurement, he started to walk back and forth. He was randomly changing his direction towards to the pole. Due to the practical limitations set by the measurement cables, anechoic chamber floor size and the antennas, the area of movement was limited to an area of approx. 1 m by 1.5 m.

IV. Data Manipulation and Selected Frequencies

The data manipulation was performed in the frequency domain by observing discrete frequencies. The time domain examination was not feasible as the demand for the channel coherence time cannot certainly be guaranteed with the used VNA sweeping time in the most mobile links examined, where the relative velocity vectors between the antennas have the highest values. However, when observing discrete frequencies, the possible problem is avoided since the Doppler frequency shift in body area measurements typically lies well below 100 Hz [15], whereas the IF bandwidth of the VNA was set to 100 kHz.

Two approaches were made. Firstly, links representing the cases where the antenna is relative constant with respect to the

TABLE I. MEASURED ANTENNA LOCATION AND TYPE COMBINATIONS

Type	Locations	Antennas
Uniform	PO-LA-LE-RE	All Dipoles or All Loops
	PO-LA-RW-LW	All Dipoles or All Loops
Mixed	PO-LA-LW-LS	Loop: LW-LS, Dipole: LA-PO or Dipole: LW-LS, Loop: LA-PO

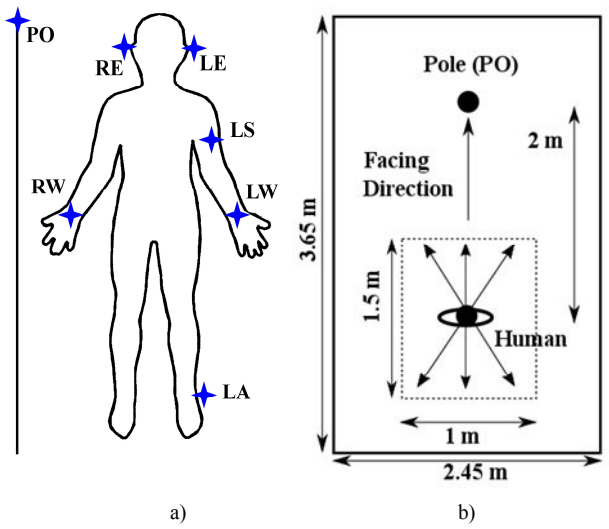

a) b)

Figure 2. a) Antenna locations b) Anechoic chamber and the test person's location and movements.

torso (LE-PO) and where their position with respect to the torso varies (LW-PO), for the uniform antenna case. They are examined at the frequencies 3496.3, 3995.0, 4493.8, 6488.8, 6987.5, 7490.0 and 7988.8 MHz corresponding closely to the center frequencies of the UWB channels 0-6 [5]. Also the frequencies 2450.0 MHz and 5798.8 MHz were included representing close the center frequencies of the 2.45 and 5.8 GHz industrial, scientific and medical bands. In addition, the frequency 3001.3 MHz serves to provide more information at the low-band UWB behavior. The diversity effect as a function of time was examined through their mirror channels (RE-PO and RW-PO) at three frequencies.

Secondly, the frequencies of 2450.0 MHz, 3995.0 MHz and 7988.8 MHz were applied to examine all measured off-body links. The frequencies 3995.0 MHz and 7988.8 MHz correspond closely to the center frequencies of the mandatory UWB low band and high band channels in [5], respectively. Both uniform and mixed antenna cases were considered.

V. RESULTS

A. Large Frequency Set with Limited Link Set

The measured data was manipulated by joining the forward and reverse channel data for each radio link under investigation, resulting 200 samples to describe the time variation of the signal. The mean values of the path loss were extracted from the linearly scaled absolute values of the data. The standard deviation σ, and the minimum and maximum values were obtained from the decibel valued data.

Fig. 3 presents the variation of the path loss as a function of time for the links LE-PO and LW-PO using uniform dipoles and for three exemplary frequencies. The presented time scale is approx. 180 seconds. It can be noted, that LE-PO has higher variation in path loss, up to 45 dB, and rate of fading is slower compared to LW-PO. It can be explained by the body shadowing effect. The antenna at the ear remains longer time in deep fade than the antenna at the wrist. The former remains quite stable with respect to the torso while the latter reaches better channel conditions more frequently with respect to the pole due to the arm movement. The small distance variation between the human and the pole during the dynamic movement has a minimal effect on the variation. The dominant effect results from the shadowing effect of the human body parts.

Within a link, when comparing the frequencies, the path loss reaches different values. One explanation to this is that the measured antenna radiation patterns in free space were noted to variate greatly as a function of frequency, direction and antenna type [14]. Furthermore, there is a minor time difference when recording the data at different frequencies. Thus, the body does not remain at exactly the same position for all frequencies.

Fig. 4 presents the path loss variation at the links RE-PO and RW-PO, representing the mirror antenna sites compared to the case in Fig. 3. It can be noted, that if, e.g., antenna diversity would be used, it may provide clear benefit to radio channel conditions. This can be seen, e.g., by comparing the LE-PO and LW-PO channels, where at high path loss time instants at one channel, the other provides often better link connection.

In Table II, the numerical data is collected at ten frequencies for the links LE-PO and LW-PO using uniform dipole antenna option. The bottom row "All" presents the

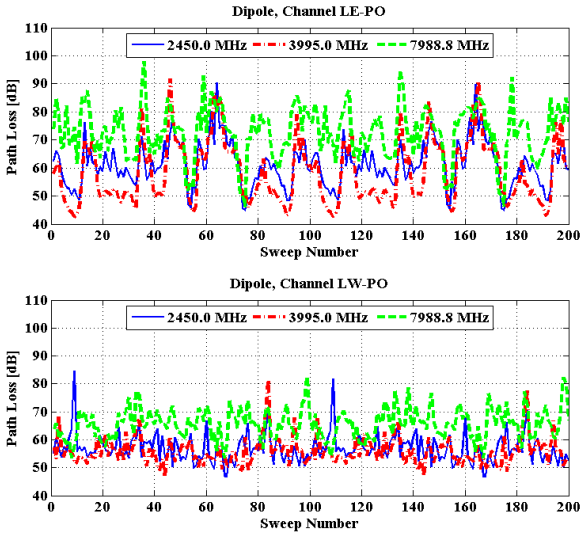

Figure 3. Path loss variation at selected frequencies for the LE-PO and LW-PO channels using dipoles.

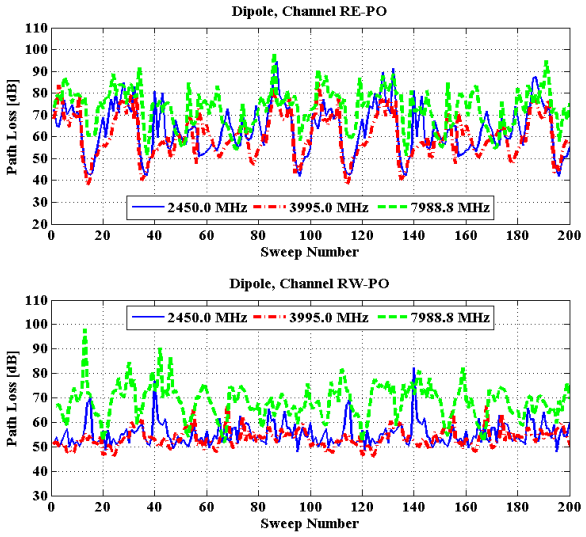

Figure 4. Path loss variation at selected frequencies for the RE-PO and RW-PO channels using dipoles.

TABLE II. PATH LOSS PARAMETERS IN THE CASE OF TEN FREQUENCIES AND THE DIPOLE ANTENNA

	Path loss parameters in dB							
Freq.	**Link LE-PO**				**Link LW-PO**			
[MHz]	***Mean***	***σ***	***Min.***	***Max.***	***Mean***	***σ***	***Min.***	***Max.***
2450.0	57.6	8.1	44.8	90.4	55.5	5.1	46.8	84.7
3001.3	54.0	8.7	42.7	79.6	56.0	6.5	45.8	81.1
3496.3	53.3	11.1	41.1	91.0	55.5	5.3	45.7	74.6
3995.0	53.1	11.0	42.5	91.8	54.6	4.9	46.9	81.6
4493.8	53.0	10.7	43.1	86.1	54.8	4.9	48.2	79.8
5798.8	57.5	9.6	41.9	89.0	61.3	6.3	52.1	81.6
6488.8	59.6	10.2	41.0	88.9	64.0	6.3	52.3	91.8
6987.5	60.4	11.2	42.7	101.7	64.3	5.9	52.3	85.6
7490.0	63.7	10.0	45.2	95.3	65.4	7.5	53.9	98.9
7988.8	66.9	9.4	46.2	98.0	63.9	5.5	53.4	82.7
All	57.9	10.0	43.1	91.2	59.6	5.8	49.8	84.3

TABLE III. PATH LOSS PARAMETERS IN THE CASE OF TEN FREQUENCIES AND THE DOUBLE LOOP ANTENNA

	Path loss parameters in dB							
Freq.	**Link LE-PO**				**Link LW-PO**			
[MHz]	***Mean***	***σ***	***Min.***	***Max.***	***Mean***	***σ***	***Min.***	***Max.***
2450.0	66.2	8.6	50.2	98.4	57.1	3.0	52.0	67.8
3001.3	59.9	8.7	44.9	87.4	50.2	2.8	45.3	61.0
3496.3	59.1	8.5	44.3	84.5	48.4	2.2	44.8	56.5
3995.0	58.5	9.1	42.7	84.9	47.6	2.7	44.1	60.8
4493.8	56.8	9.7	41.2	84.8	48.6	2.7	44.5	60.3
5798.8	60.5	10.4	43.9	94.1	55.6	3.3	50.3	71.5
6488.8	58.2	12.2	40.6	93.8	57.4	4.8	49.3	79.5
6987.5	61.1	13.1	43.3	102.0	60.3	5.9	51.6	80.9
7490.0	66.3	11.2	45.4	100.2	59.7	5.3	50.0	78.7
7988.8	66.9	10.4	48.7	99.2	60.8	4.5	54.4	78.3
All	61.3	10.2	44.5	92.9	54.6	3.7	48.6	69.5

average value of all frequencies. The mean path losses vary between 53.0-63.9 dB. The path loss is higher with LW-PO in eight frequencies out of ten. LE-PO has higher maximum path loss in seven cases out of ten ranging between 79.6-101.7 dB. The standard deviation is higher for LE-PO, which is visible also in Fig. 3.

Table III contains corresponding data when uniform double loops are used. The mean and maximum path losses are in all cases higher with LE-PO. When comparing dipole and double loop antennas, it can be noted that the mean path loss is higher with the double loop in LE-PO, but lower in LW-PO. One reason to this is that the antenna locations and the test person movements cannot be identical between different measurements.

B. Large Link Set with Limited Frequency Set

Table IV contains results in the case, when the frequency set is limited to three, and all links are considered. The mean values of the path loss and standard deviation are shown. The data is presented for both antenna types. For the dipole, the path loss varies between 52.7-67.9 dB with a standard deviation of ranging between 3.8-11.3 dB. The highest deviations exists at the links LE-PO and RE-PO and the lowest ones with LW-PO and RW-PO. The differences in path losses between links in a single frequency is at maximum approx. 10 dB. When comparing the frequencies in pairs, e.g., 2450.0 MHz/3995.0 MHz, 2450.0 MHz/7988.8 MHz and 3995.0/7988.8 MHz, it is noted that in 11 cases out of 15 the path loss increases with the frequency.

In the loop antenna case, the path loss variates between 47.6-69.4 dB with σ between 2.5-10.4 dB. As with dipole, the most stable links are LW-PO and RW-PO and the largest variation exists at LE-PO and RE-PO. When comparing the antennas, in seven cases out of 15, the dipole has higher path loss than the double loop. Therefore, it cannot be stated which antenna performs better based on the tabulated data.

Table V shows the results when using mixed antennas. The links with mixed antenna pairs are LW-PO and LS-PO. The path loss reaches values between 51.3-65.2 dB. Therefore, using different antenna types does not have any remarkable impact on the results.

TABLE IV. PATH LOSS PARAMETERS IN ALL LINKS CASE FOR BOTH UNIFORM ANTENNA CASES

		Dipole			**Double Loop**		
		Freq. [MHz]			**Freq. [MHz]**		
Link	***[dB]***	***2450.0***	***3995.0***	***7988.8***	***2450.0***	***3995.0***	***7988.8***
LA-PO	***Mean***	55.1	63.6	69.1	64.7	69.4	67.3
	σ	8.5	7.3	8.3	6.5	6.6	6.7
LE-PO	***Mean***	57.6	53.1	66.9	66.2	58.5	66.9
	σ	8.1	11.0	9.4	8.6	9.1	10.4
RE-PO	***Mean***	56.6	54.8	67.9	60.3	50.5	60.9
	σ	11.3	10.3	9.3	4.4	5.3	6.7
LW-PO	***Mean***	55.5	54.6	63.9	57.1	47.6	60.8
	σ	5.1	4.9	5.5	3.0	2.7	4.5
RW-PO	***Mean***	54.1	52.7	65.4	59.7	48.7	62.0
	σ	4.8	3.8	7.1	3.9	2.5	6.7

TABLE V. PATH LOSS PARAMETERS IN THE MIXED ANTENNA AND ALL LINKS CASE

		Loop: LS and LW Dipole: LA and PO			**Dipole: LS and LW Loop: LA and PO**		
		Freq. [MHz]			**Freq. [MHz]**		
Link	***[dB]***	***2450.0***	***3995.0***	***7988.8***	***2450.0***	***3995.0***	***7988.8***
LW-PO	***Mean***	57.7	54.8	64.6	56.1	51.3	55.1
	σ	7.6	5.3	8.1	5.9	3.3	5.8
LS-PO	***Mean***	58.9	53.2	65.2	62.7	52.4	56.5
	σ	8.1	6.5	7.8	7.1	4.9	5.9
LA-PO	***Mean***	54.9	60.7	67.6	57.5	64.9	65.9
	σ	7.9	6.7	7.3	6.5	6.9	7.6

VI. CONCLUSIONS AND FUTURE WORK

The paper reports the results from measurements of dynamic off-body radio channels at UWB frequencies extending the knowledge of the shadowing effect present in the dynamic scenario. The results are conducted in an anechoic chamber to investigate the human body shadowing effect. Six antenna locations were selected on the body, and one antenna was installed off the body. Two antenna types were applied, dipole and double loop.

First, two links and ten frequencies were selected to analyze the effect of frequency in detail. The path loss parameters were found out. Secondly, all measured links were considered at three frequencies. The mean path loss varies between 47.6-69.4 dB depending on the link, frequency and antenna type. The maximum path loss was 101.7 dB, and the minimum 44.1 dB. No clear difference can be noted between the antennas. Furthermore, the usage of dipole and double loop as a pair has no notable effect compared to the case when the antennas are similar. Therefore, the antenna types have no significant role in the analysis of the channel data in this paper.

In the future, more measurements should be conducted with respect to more antenna locations, and different environments. Statistical models will be developed with a larger amount of data. The classical information to describe temporal variation of radio channels, e.g., level crossing rate and average fade duration, will be uncovered.

REFERENCES

[1] P. S. Hall and Y. Hao, Antennas and Propagation for Body-Centric Wireless Communications, 2nd ed., Norwood, MA, Artech House, 2012, pp. 1-16.

[2] United Nations, Department of Economic and Social Affairs, World Population Ageing 2017 (accessed in January 2019), [Online]. Available: http://www.un.org/en/development/desa/population/publications/pdf/ageing/WPA2017_Highlights.pdf.

[3] I. Oppermann, M. Hämäläinen, J. Iinatti (eds.), UWB Theory and Applications. West Sussex, England, John Wiley & Sons, 2004, pp. 1-7.

[4] M. Ghawami, L.B. Michael and R. Kohno, Ultra Wideband Signals and Systems in Communication Engineering, Second Edition, West Sussex, England, John Wiley & Sons, 2007, pp. 1-24.

[5] IEEE standard for local and metropolitan area networks, IEEE 802.15.6-2012 – Part 15.6: wireless body area networks, 2012.

[6] R.-G. Garcia-Serna, C. Garcia-Pardo, and J. Molina-Garcia-Pardo, "Effect of the receiver attachment position on ultrawideband off-body channels," IEEE Antennas Wireless Propag. Lett., vol. 14, 2015, pp. 1101-1104.

[7] T. Kumpuniemi, J.-P. Mäkelä, M. Hämäläinen, K. Yekeh Yazdandoost, and J. Iinatti, "Human body effect on static UWB WBAN off-body radio channels," in Proc. 13th Int. Conf. on Body Area Networks (BodyNets), Oct. 2018, Oulu, Finland, pp. 1-10.

[8] M. M. Khan, Q. H. Abbasi, A. Alomainy, Y. Hao, and C. Parini, "Experimental characterization of ultra-wideband off-body radio channels considering antenna effects," IET Microw. Antennas Propag., vol. 7, iss. 7, 2013, pp. 370-380.

[9] T. Kumpuniemi, J.-P. Mäkelä, M. Hämäläinen, K. Yekeh Yazdandoost, and J. Iinatti, "Dynamic UWB off-body radio channels - human body shadowing effect,", in Proc. 28th Ann. IEEE Int. Symp. on Personal, Indoor and Mobile Radio Commun. (PIMRC), Oct. 2017, Montreal, Canada, pp. 1-7.

[10] T. Kumpuniemi, M. Hämäläinen, K. Yekeh Yazdandoost, and J. Iinatti, "Categorized UWB on-body radio channel modeling for WBANs," Progress in Electromagnetic Research B, vol. 67, 2016, pp. 1-16.

[11] T. Kumpuniemi, M. Hämäläinen, K Yekeh Yazdandoost, and J. Iinatti, "Human body shadowing effect on dynamic UWB on-body radio channels," IEEE Antennas Wireless Propag. Lett., vol. 16, 2017, pp. 1-4.

[12] T. Tuovinen, T. Kumpuniemi, K. Yekeh Yazdandoost, M. Hämäläinen, and J. Iinatti, "Effect of the antenna-human body distance on the antenna matching in UWB WBAN applications," in Proc. 7th Int. Symp. on Medical Inform. and Commun.Technology (ISMICT), March 2013, Tokyo, Japan, pp. 193-197.

[13] T. Tuovinen., T. Kumpuniemi, M. Hämäläinen., K. Yekeh Yazdandoost, and J. Iinatti, "Effect of the antenna-body distance on the on-ext and on-on channel link path gain in UWB WBAN applications," in Proc. 35th Annu. Int. Conf. IEEE Eng. in Medicine and Biology Society (EMBC), July 2013, Osaka, Japan, pp. 1242-1245.

[14] T. Kumpuniemi, M. Hämäläinen, K. Yekeh Yazdandoost, and J. Iinatti, "Measurements for body-to-body UWB WBAN radio channels," in Proc. 9th Eur. Conf. on Antennas and Propag. (EUCAP), 2015, pp. 1-5.

[15] R. Fu, Y. Ye, N. Yang, and K. Pahlavan, "Doppler spread analysis of human motions for body area network applications," in Proc. IEEE 22nd Int. Symp. on Personal, Indoor and Mobile Radio Commun. (PIMRC), Sept. 2011, Toronto, Canada, pp. 2209-2213.